



HAL
open science

Scratching and transplanting of electro- active biofilm in fruit peeling leachate by ultrasound: re-inoculation in new microbial fuel cell for enhancement of bio- energy production and organic matter detection

Hakima Kebaili, Mostéfa Kameche, Christophe Innocent, Amina Benayyad,
Widya Ernayati Kosimaningrum, Tewfik Sahraoui

► To cite this version:

Hakima Kebaili, Mostéfa Kameche, Christophe Innocent, Amina Benayyad, Widya Ernayati Kosimaningrum, et al.. Scratching and transplanting of electro- active biofilm in fruit peeling leachate by ultrasound: re-inoculation in new microbial fuel cell for enhancement of bio- energy production and organic matter detection. *Biotechnology Letters*, 2020, 42 (6), pp.965 - 978. 10.1007/s10529-020-02858-5 . hal-02570145

HAL Id: hal-02570145

<https://hal.science/hal-02570145>

Submitted on 9 Dec 2020

HAL is a multi-disciplinary open access archive for the deposit and dissemination of scientific research documents, whether they are published or not. The documents may come from teaching and research institutions in France or abroad, or from public or private research centers.

L'archive ouverte pluridisciplinaire **HAL**, est destinée au dépôt et à la diffusion de documents scientifiques de niveau recherche, publiés ou non, émanant des établissements d'enseignement et de recherche français ou étrangers, des laboratoires publics ou privés.



Scratching and transplanting of electro-active biofilm in fruit peeling leachate by ultrasound: re-inoculation in new microbial fuel cell for enhancement of bio-energy production and organic matter detection

Hakima Kebaili · Mostefa Kameche · Christophe Innocent · Amina Benayyad · Widya Ernayati Kosimaningrum · Tewfik Sahraoui

Received: 25 September 2019 / Accepted: 29 February 2020
© Springer Nature B.V. 2020

Abstract

Objective An electro-active biofilm of Fruit Peeling (FP) leachate was formed onto the Carbon Felt (CF) bio-anode in a Microbial Fuel Cell (MFC), after functioning for a long time. The electro active-biofilm thus formed was then scratched by ultrasound and re-inoculated in a new leachate to be transplanted onto the bio-anode. This procedure allowed the microbial electron charge transfer and therefore the enhancement of the bio-energy production of the fuel cell.

Results By using the repetitive mechanical biofilm removal, re-suspension and electrochemically facilitated biofilm formation, the voltage was substantially increased. In effect, the voltage of the 1st G of biofilm, rose gradually and reached its maximum value of

65 mV after 10 days. Whilst the 2nd generation allowed to obtain the maximum voltage 276 mV and without any lag time. The DCO abatement using the 1st G biofilm was 68% greater than the 3rd G 26%. Besides, the electrochemical impedance spectroscopy characterization and cyclic voltammetry of bio-anode with 2nd G biofilm confirmed the ability of electro-active biofilm formation on a new support. The biofilm transplanted showed thus greater kinetic performance, with reduced lag time demonstrating the interest of the selection that took place during the formation of successive biofilms.

Conclusions Despite the transplantation of the electro-active biofilm onto the bio-anode, the MFC still

H. Kebaili · M. Kameche (✉) · A. Benayyad
Laboratory of Physico-Chemistry of Materials, Catalysis and Environment, University of Sciences and Technology of Oran, Mohammed-Boudiaf, Oran, Algeria
e-mail: kameche@hotmail.com
mostefa.kameche@univ-usto.dz

H. Kebaili
e-mail: hakima.kebaili@univ-usto.dz;
kebailihakima@gmail.com

A. Benayyad
e-mail: benayyadlamina@gmail.com

H. Kebaili · M. Kameche · C. Innocent ·
W. E. Kosimaningrum
European Institute of Membranes,
University of Montpellier, Montpellier, France
e-mail: christophe.innocent@umontpellier.fr

W. E. Kosimaningrum
e-mail: widya_ernayati@yahoo.com

W. E. Kosimaningrum
Analytical Chemistry Division, Faculty of Mathematics and Natural Science, Institute of Technology Bandung, Bandung, Indonesia

T. Sahraoui
Laboratory of Electronic Microscopy and Materials Science, University of Sciences and Technology of Oran, Mohammed-Boudiaf, Oran, Algeria
e-mail: sahraoui_tewfik1@yahoo.fr

39 produced relatively lower power output. Nevertheless,
40 it has been tested successfully for monitoring and
41 detecting the oxidation of sodium acetate substrate in
42 the very wide concentration range 0.0025–35 g/l.

43 **Keywords** Carbon felt · Microbial fuel cell ·
44 Electroactive bio-film · Scratching-transplantation ·
45 Acetate detection

Abbreviations

| | | |
|----|--------|---|
| 46 | CF | Carbon felt |
| 47 | CG | Carbon graphite |
| 48 | GS | Garden soil |
| 49 | GS-MFC | Garden soil microbial fuel cell |
| 50 | FP | Fruit peeling |
| 51 | FP-MFC | Fruit peeling microbial fuel cell |
| 52 | 1st | First generation microbial fuel cell |
| 53 | G-MFC | |
| 54 | 1st G | First generation biofilm |
| 55 | 2nd G | Second generation biofilm (re-inoculated biofilm) |
| 56 | 3rd G | Third generation biofilm (re-inoculated biofilm) |
| 57 | MFC | Microbial fuel cell |
| 58 | SS | Stainless steel |
| 59 | Gs | Generations |

Introduction

63 Owing to preservation of environment, industrial
64 wastewaters that contain a great deal of organic
65 matter, require stronger treatment (Mathuriya and
66 Sharma 2009). In general, managers of industrial units
67 choose the promising low cost technology of Micro-
68 bial Fuel Cells (MFCs), for the treatment of their
69 effluents (Huang and Logan 2008). These innovative
70 electrochemical devices, convert organic wastes into
71 electricity by oxidation (Tingry et al. 2013).

72 A MFC consists of two compartments (anodic and
73 cathodic) separated by a cation exchange membrane.
74 In the anodic compartment, the micro-organisms form
75 the biofilm that oxidises the organic matter, known as
76 biocatalyst (Santoro et al. 2017). Whilst, the cathodic
77 compartment uses metal or nano-particles catalysts
78 such as platinum, nickel, etc...., to reduce oxygen.
79 Moreover, these devices need rich environment of

great microbial diversity that can convert different 80
organic compounds into sustainable and renewable 81
energy. 82

83 Performance optimisation of MFC for wastes
84 treatment and sustainable clean energy generation
85 was investigated to make easier the commercialisation
86 of this new technology (Sedighi et al. 2018). Amongst
87 the innovative applications utilizing MFCs, we can
88 cite the treatment of domestic wastewaters (Puig et al.
89 2011), the reduction of sludge produced by biological
90 treatment (Kim et al. 2007), treatment of diary
91 industrial effluent (Manohar et al. 2008), and more
92 recently biotreatment of vinasse (Ottoni et al. 2019),
93 removal of salts and elimination of heavy metals traces
94 from wastewater (Champavert et al. 2017; Yahiaoui
95 et al. 2020).

96 Upon the oxidation of organic matter by biofilm
97 (bio-catalyst), three mechanisms between the bacterial
98 population and electrodes, can occur: Direct transfer
99 using cytochromes (Holmes et al. 2004; Cheng et al.
100 2006; Fapetu et al. 2016); indirect transfer using
101 mediators either exogen or endogen, such as dyes
102 (Nam and Park 1999) and phenazines (Rabaey et al.
103 2004) and finally electron transfer by means of
104 nanowires (Gorby et al. 2006).

105 The biofilm formation mechanisms in electro active
106 microorganisms leading to improved electrocatalytic
107 rates for applications in bioelectrochemical systems,
108 were addressed (Angelaalincy et al. 2018). The screen-
109 ing of sediment and wastewater samples to be used as
110 anolytes in a MFC for microbial electron transfer
111 activity, was recently investigated (Aiyer et al. 2019).
112 The inoculation of a reactor with a scraped-off biofilm
113 collected from a running MFC, improved the electro-
114 chemical performance of the new biofilm with respect
115 to that was used as inoculum (Cheng et al. 2011). The
116 successive scratching and re-inoculation steps using
117 lower polarisation potentials, showed an increase in
118 current density using paper waste MFC (Ketep et al.
119 2013). The consecutive selection and acclimatization
120 of wastewater inoculum based, mixed culture micro-
121 bial biofilms demonstrated an alternative biofilm
122 removal, re-suspension and electrochemically facili-
123 tated biofilm formation.

124 It was shown that the bio-electrocatalytic current
125 density of the secondary biofilm formation was much
126 greater than a primary biofilm in a MFC (Liu et al.
127 2008). Furthermore, it has been demonstrated that
128 once a biofilm was formed on a given anode (1st G),

129 then was transferred to a new sterile leachate and made
130 in contact with a new electrode support, it continued to
131 grow allowing the formation of the 2nd G (Rivalland
132 et al. 2015). Moreover, the biofilm transfer can be
133 achieved by suspension of the support-electrode in
134 buffered solution, handshaking and scraping of any
135 remaining biofilm (Kim et al. 2014).

136 In view of this bibliography, we followed the
137 scratching/transplanting method utilized by Ketep
138 et al. (2013) using two different backgrounds: garden
139 ^{AQ1}soil and natural fruit peeling leachates, for comparing
140 and testing the advantage of biofilm re-inoculation. In
141 effect, we tested the benefits of re-inoculation of
142 bacterial biofilm formed on electrode surfaces using
143 fuel cell device without prior polarization of bio-
144 anode. The purpose of the present paper was to
145 perform the scratching/re-inoculation of bacterial
146 biofilm, for increasing bio-energy of MFC and
147 ^{AQ2}oxidizing organic matter contained in wastewater.
148 We characterized the three successive biofilm gener-
149 ations by Scanning Electronic Microscopy (SEM),
150 Cyclic Voltammetry (CV) and Electrochemical Impe-
151 dance Spectroscopy (EIS). Besides, despite its lower
152 power output, we utilized this MFC for monitoring and
153 detecting the oxidation of sodium acetate in a very
154 ^{AQ3}wide concentration range. Finally, we assessed the
155 current response of the MFC-based detector to various
156 concentrations of substrate in the effluent.

157 Experimental

158 Inoculum and microbial fuel cell

159 Effluent samples were prepared from 500 g of Fruit
160 Peelings (FP) mixed with potassium chloride solution
161 60 mM (conductivity = 8.85 mS cm⁻¹ and pH 4.8).
162 Another leachate was prepared similarly using Garden
163 Soil (GS) (conductivity = 11.72 mS cm⁻¹ and pH
164 5.2). They were used without further filtration as
165 inoculum source for microbial reactor.

166 As illustrated by Fig. 1a, the MFC consisted of two
167 glass spherical half-cells 75 mL, connected to each
168 other by cationic exchange perfluorinated membrane
169 (Nafion-117; Dupont, Ward Hill, MA, USA), 2 cm in
170 diameter. The Carbone Felt (CF) and Stainless Steel
171 (SS) sheet were used as bio-anode and cathode
172 respectively. They were thus, placed inside the anolyte
173 and catholyte of the MFC. The anolyte contained the

leachate fed continuously with sodium acetate solu- 174
tion (20 mM), whereas the catholyte contained potas- 175
sium ferricyanide K₃[Fe(CN)₆] 20 mM. The top end 176
of the anolyte was tightly sealed with paraffin film to 177
reduce oxygen penetration. Owing to polarization and 178
in order to render the biofilm electroactive, an external 179
resistor (1000 Ω) to complete a closed external circuit 180
loop and Copper wires were used to conduct electrons 181
between electrodes. The electroactive biofilm was 182
therefore formed on the surface of the electrode within 183
10 days and the evolution of the cell voltage with time, 184
was then measured with the digital voltmeter (APRI- 185
LIA M890C+) placed in parallel. 186

Scratching/transplanting biofilm 187

The aim of the present investigation was to select the 188
electro-active bio-film and to eliminate the non- 189
electroactive bacterial species that consumed the fuel 190
uselessly without producing any valuable energy. 191

In our experiments, the successive biofilm were 192
formed in the FP effluent which was sterilized to 193
remove planktonic microorganisms. As a matter of 194
fact, the primary biofilm was formed from FP leachate 195
in running MFC. It was then scratched-off from the 196
bioanode by ultrasound and used as inoculum in 197
another MFC to form the secondary biofilm. Besides, 198
in order to optimize the operating conditions for 199
electroactive biofilm development, and stabilize the 200
substrate, sterilized sodium acetate solution was added 201
daily. Under this condition, the pH of the bulk was 202
controlled by the evolution of the effluent itself. The 203
experimental protocol was compared to others, for 204
allowing the formation of the primary biofilm. 205

In reference to literature, we review below the 206
previous methods so far utilized for scratching and 207
transplanting of electro-active bio-film onto carbon 208
carbon-based materials, which are as follows: 209

a-As suggested by Rivalland et al. (2015), the 210
biofilm formed on an anode (in 1st G), it was then 211
transferred to a new sterile leachate and made in 212
contact with a new electrode support. It resulted in the 213
growth of the 2nd G biofilm. The same procedure was 214
followed to form the 3rd G biofilm generation. 215

b-As recommended by Kim et al. (2014), and Doyle 216
et al. (2017), the biofilm transfer can be achieved by 217
suspension of the support-electrode in buffered solu- 218
tion, handshaking and scraping of any remaining 219
biofilm. 220

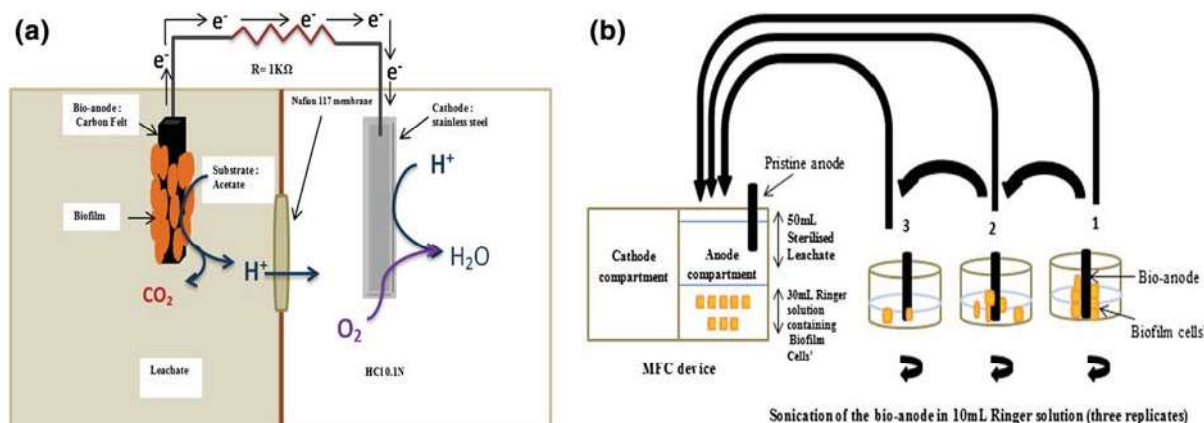


Fig. 1 a Scheme of MFC, b sonication method steps

221 c-As advised by Ketep et al. (2013) and Yates et al.
 222 (2017), the primary biofilm was scrapped-off from
 223 bio-anode using sonication in Ringer solution, then
 224 transferred into sterilized leachate to be re-inoculated
 225 onto a new electrode.

226 Accordingly, we adopted in the present work the
 227 method followed by Ketep et al. (2013). In effect, after
 228 forming the electro-active biofilm in the MFC, the
 229 electrode bearing this biofilm was subject to sonica-
 230 tion suspended in Ringer's solution (30 ml) for 15 min
 231 in three replicates, 5 min each in order to preserve the
 232 bacterial cells already scratched. This makes it possi-
 233 ble to recover more cells without exposing the
 234 unhooked cells to a long duration of sonication
 235 (Fig. 1b). The primary biofilm was formed onto CF
 236 bio-anode in MFC during more than ten days without
 237 supplying any electrical polarisation. The biofilms
 238 formed from the successive re-inoculations were then
 239 performed in identical experimental conditions.

240 The primary electroactive biofilm formed in 1st
 241 MFC, was detached from the initial inoculated elec-
 242 trode by ultrasound in 30 ml physiological sterilised
 243 Ringer solution. This volume was added to a new
 244 sterilized leachate to be inoculated and used as the
 245 anodic chamber for a new electrochemical cell called
 246 2nd MFC. The primary biofilm were removed from the
 247 anode surface and used to inoculate a new electro-
 248 chemical reactor filled with sterilized FP leachate. The
 249 new biofilm (i.e. 2nd G) was formed on the new
 250 sterilised carbon felt electrode: the same steps were
 251 followed to form 3rd G.

252 The scanning electron microscope JSM-6610LA
 253 was used to examine the anodic electrode surface

before the MFC experiment and after the biofilm re-
 254 formation. 255

256 *Electrochemical characterisation*

257 The cyclic voltammetry curves were recorded at scan
 258 rate 10 mV/s and electrochemical impedance spec-
 259 troscopy diagrams were recorded in range (100 kHz to
 260 100 mHz) using the potentiostat-galvanostat (PGZ-
 261 301). The temperature was maintained at 25 °C. The
 262 electrochemical glass cells of 80 mL were filled with
 263 FP leachate containing primary biofilm (1st G),
 264 secondary (2nd G) or tertiary biofilm (3rd G). The
 265 lid and the reactor-body were sealed with a clamping
 266 ring. The working electrodes were flat 1.27 cm in
 267 diameter and 5 cm in length CF (99%, Alfa Aesar)
 268 screwed onto 5 mm diameter, 1 cm long graphite rods
 269 that ensured the electrical connection. The new CF
 270 electrodes were pre-treated by soaking in hydrochloric
 271 acid 1.0 M overnight to eliminate possible metal ion
 272 contamination, 20 min rinsing with distilled water (10
 273 times) then immersed in sterilized water 48 h and
 274 allowed to dry in an oven (50 °C) at least one hour.
 275 Auxiliary electrodes were stainless steel flat cleaned
 276 by sterilization in Pasteur oven (Heraeus INSTRU-
 277 MENTS Vacutherm). Potentials were controlled and
 278 expressed versus a saturated silver chloride electrode.
 279 The working electrode (i.e. bio-anode) was kept as
 280 close as possible to the reference electrode in front of
 281 the platinum auxiliary electrode.

282 **Results**

283 Voltage evolution of MFCs

284 In previous investigations, the first 1st G of biofilm
 285 was obtained naturally by connecting directly the bio-
 286 anode to cathode in closed circuit configuration using
 287 an electric resistance (Huang et al. 2014; Cabezas et al.
 288 2015). Accordingly, the same procedure was, there-
 289 fore followed by us to obtain the 1st G of biofilm,
 290 where the voltage increased gradually and reached its
 291 maximum value of 65 mV after 10 days. As for the
 292 2nd G, the voltage started with 150 mV without lag
 293 time and attained its highest value of 276 mV.
 294 However, the voltage of the 3rd G was lower than
 295 that of the 2nd G but was still higher than the 1st G.

296 By comparing the temporal progression (Fig. 2) of
 297 MFCs using the electrodes of the 1st and 2nd Gs, the
 298 following comments may be made:

- 299 • During the first period (0–100 h), the MFC of 2nd
 300 G allowed a starting voltage greater than 10 mV,
 301 right up the 1st hour, which explained the rapid
 302 formation of electroactive biofilm in the presence
 303 of the 1st G biofilm scratched (tested in sterile
 304 environment and electrode). Between 100 and
 305 200 h, the improvement of the voltage of the 1st G
 306 MFC was noticed, due to the formation of the
 307 electroactive biofilm. After 200 h, the variations of
 308 the voltage of the two MFCs were identical which
 309 resulted in the stable formation of the electro-
 310 active biofilm on both electrodes.
- 311 • Throughout 10 days, the temporal variations of the
 312 three generations show that the FP-MFC of the 2nd

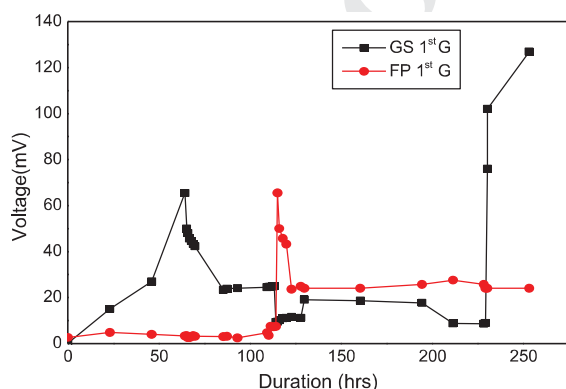


Fig. 2 Evolution voltage curves of 1st G MFC using: GS and FP leachates

G recorded an initial electric voltage higher than 313
 5 mV and a rapid progression from the second 314
 operating day (Table 1). There was an increase of 315
 the cell voltage, upon the addition of the fuel. 316
 Really, the voltage was much higher, when the 317
 medium had been changed and the fuel had been 318
 added simultaneously. 319

Moreover, the two MFCs of 2nd G (GS and PF) 320
 have been compared between each other. For both 321
 MFCs, an initial voltage greater than 5 mV was 322
 observed with a rapid progression from the second 323
 operating day. In addition, during the voltage evolu- 324
 tion, two antagonist behaviours were observed. The 325
 GS-MFC (1st G) started right up from the beginning, 326
 whilst the FP-MFC did so after 5 days. For the 2nd G 327
 (i.e. after biofilm transplantation), the opposite 328
 occurred, showing a remarkable difference in lag time 329
 of 2 days for GS-MFC (Fig. 3). 330

Primary, secondary and tertiary biofilms formed 331
 in MFC 332

Akoğlu (2020) have recently carried out an investiga- 333
 tion on the biofilm formation obtained from lactic acid 334
 bacteria. The biofilm was utilized advantageously and 335
 beneficially as the starter culture, for the formation of 336
 the new biofilm. On this basis, our primary biofilm 337
 collected from a MFC prototype, was removed from 338
 the anode surface by ultrasound and was then used to 339
 inoculate a new electrochemical reactor filled of 340
 sterilized FP leachate. As shown in Fig. 4, the new 341
 biofilm (2nd G) was therefore formed on the new 342
 sterilized CF electrode. The initial lag period was in 343
 contrast reduced with respect to that obviously 344
 observed with the primary biofilm; the bioenergy 345
 performances were thus amply better. Consequently, 346
 the secondary biofilm was used to inoculate the third 347
 electrochemical reactor. The 3rd G showed a 348

Table 1 Values of voltage (mV) of FP-MFC

| Duration (h) | Sterilized leachate | 1st G | 2nd G | 3rd G |
|--------------|---------------------|-------|-------|-------|
| 33 | < 1 | 5 | 150 | 52.2 |
| 66 | < 1 | 65 | 201.3 | 82 |
| 266 | < 1 | 20 | 276 | 220 |

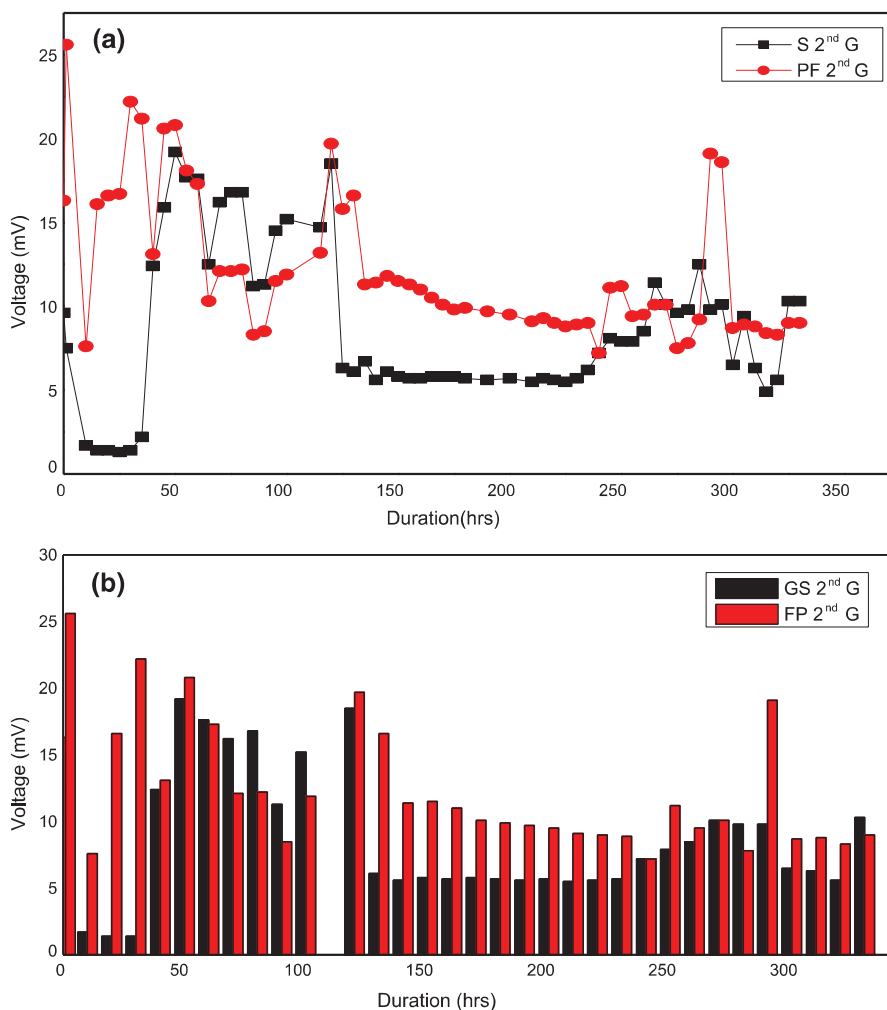


Fig. 3 Comparison between 2nd electricity generation GS and FP MFCs; **a** evolution curves and **b** bar-chart values

349 remarkable performance as well; it provided maxi-
350 mum power density about 21.77 mW m^{-2} .

351 In summary, forming the primary biofilm as
352 inoculum led to the secondary biofilm that provided
353 the significant power density which was four times
354 higher than that given with the primary biofilm
355 (Fig. 5). It was besides possible to form the tertiary
356 biofilm from the secondary biofilm as inoculum. The
357 power density yielded with the tertiary biofilm was
358 slightly lower than that observed with the secondary
359 one. These results are in quite good agreement with
360 previous investigations in the improvement of bio-
361 electro-catalytic performance of mixed culture bio-
362 films by consecutive electrochemical selection. A
363 comparison of primary and secondary biofilms

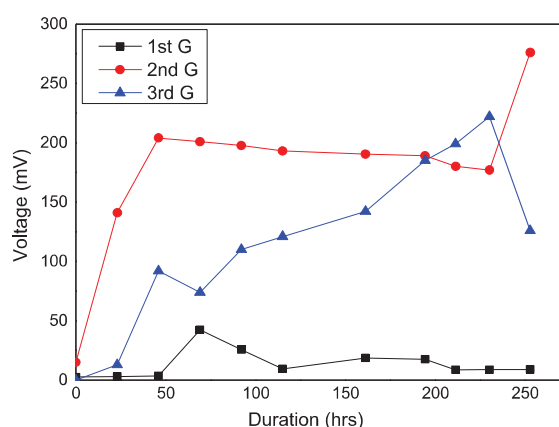


Fig. 4 Evolution voltage curves of FP-MFCs: 1st G; 2nd G and 3rd G

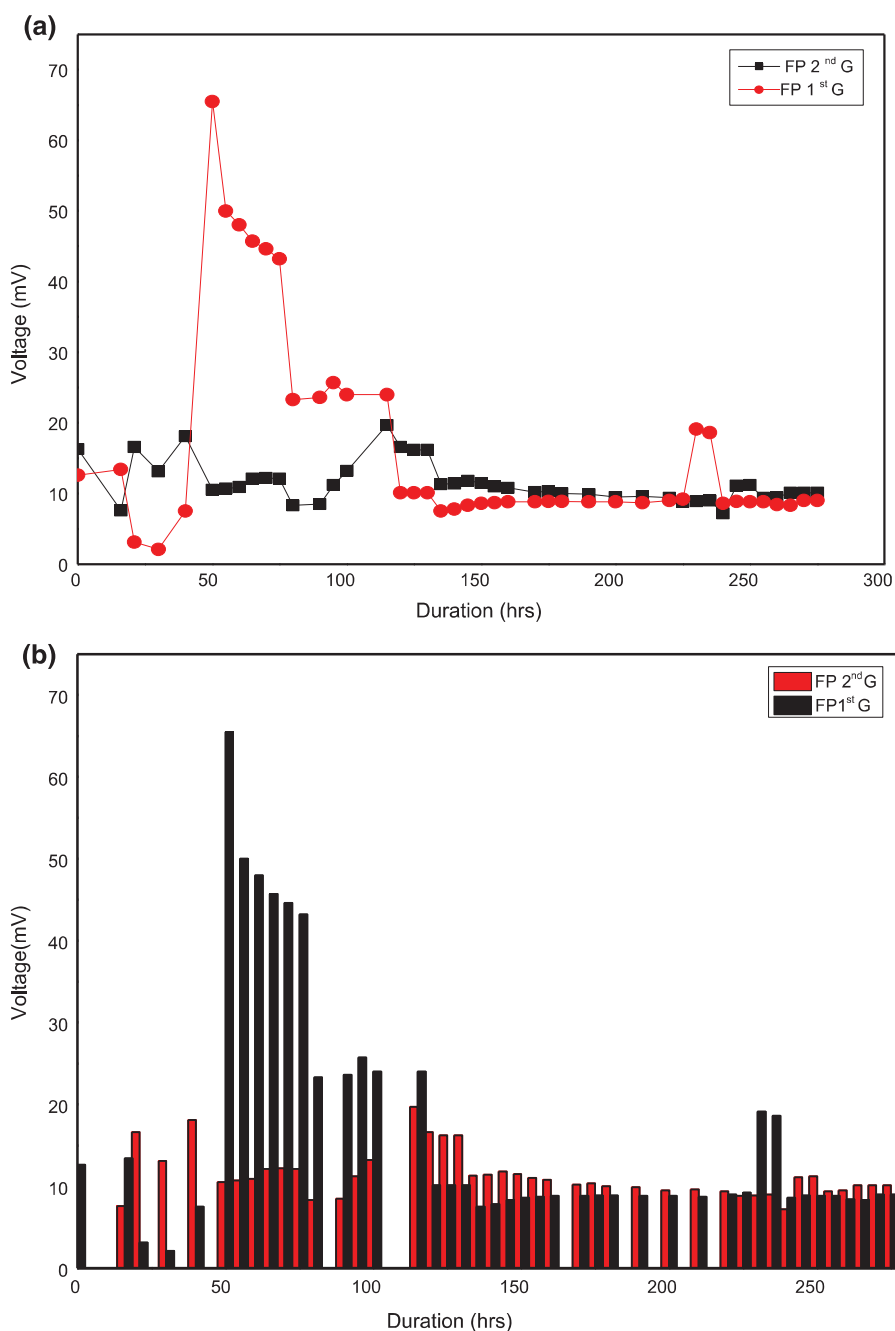


Fig. 5 Comparison between FP-MFCs of 1st and 2nd Gs; **a** Evolution curves and **b** Bar-chart values

364 revealed that the secondary biofilm usually exceeds
 365 the primary one (Liu et al. 2008).

366 Furthermore, as shown in Fig. 6, SEM images
 367 (magnification 50 μ m) confirm reformation of bio-
 368 films resulting from sonication of successive FP
 369 generations: a) pristine CF fibres, b) biofilm of 1st

G, c) biofilm of 2nd G, d) biofilm of 3rd G. 370
 Qualitatively, the scratching/transplanting of our 371
 biofilm by ultrasound seems to be in agreement with 372
 the experience described by Zhao et al. (2015), where 373
 it was shown that delaying polarization of carbon cloth 374
 bioanode, brought about biofilm architecture that was 375

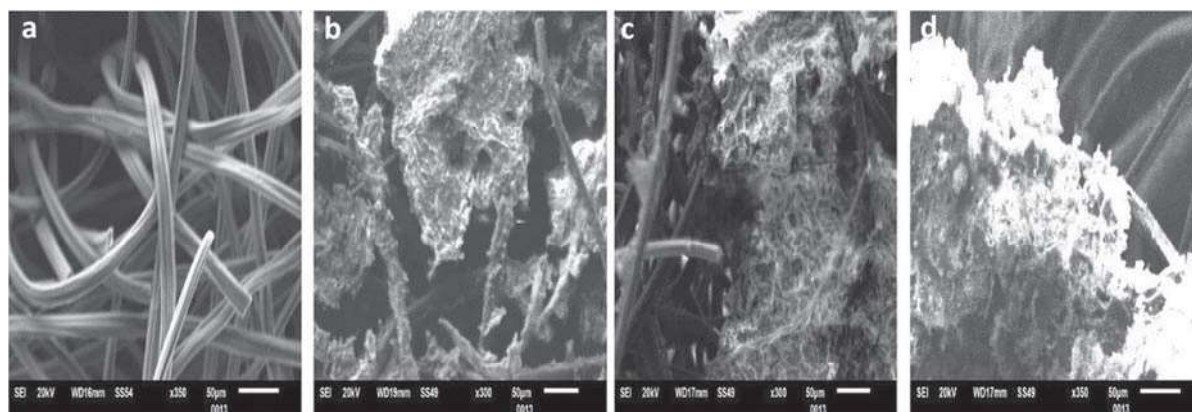


Fig. 6 SEM images (magnification 50 μm) confirm reformation of biofilms resulting from sonication of successive generations: **a** pristine CF; **b** biofilm of 1st G; **c** biofilm of 2nd G; **d** biofilm of 3rd G

376 more heterogeneous and thinner as compared to
377 homogenous and thick biofilm resulting in full
378 polarization.

379 Electrochemical characterization

380 *Impedance spectroscopy*

381 The impedance spectra of the different MFCs are
382 represented according to the Nyquist diagram. They
383 are represented in Fig. 7 given below, for the different
384 electrodes (pristine, 1st G, 2nd G and 3rd G). In
385 general, their shapes are semi-circles which intersect
386 the axis of the real at the two points R_e and R_{tc}
387 corresponding to the electrolyte and transfer resis-
388 tances respectively. Obviously, the variations of the
389 curves are different, reflecting the duration of opera-
390 tion of the MFC, in the presence of the bacterial
391 biofilm. However, the MFC without biofilm has the
392 highest resistance, the pristine work electrode gives a
393 relatively higher resistance, and finally that of the 3rd
394 G has the lowest resistance due to the electro-activity
395 of the bacterial biofilm where the electronic conduc-
396 tion is better. This theory is verified in the case of
397 electrodes immersed in the juice solution of autumn
398 peelings fruits. For GS leachate, the electrode carrying
399 the biofilm of the 1st G has a higher resistance than the
400 electrode of the 2nd G: it is assumed in this case that
401 the electroactive biofilm has not taken enough time to
402 rebuild itself for train the 2nd G. In order to make it
403 clear, a zooming has been provided inside the

figure where the curves overlapped. The values of
real impedance of the three generations and the
pristine electrode are therefore in the following order:

$$\text{Re}(Z)_{3\text{rd G}} < \text{Re}(Z)_{2\text{nd G}} < \text{Re}(Z)_{1\text{st G}} < \text{Re}(Z)_{\text{pristine}}$$

As it is shown by the above inequalities, the thicker
and fully developed the electroactive biofilm, the
lower the charge transfer resistance was. The biofilm-
free MFC yields the highest resistance, the sterile
gives a relatively lower resistance, and finally the third
generation leads to the lowest resistance due to the
electro-activity of the bacterial biofilm where elec-
tronic conduction becomes much pronounced. Qualita-
tively, our results are comparable to those previously
reported by Doyle et al. (2017), though they used
polarization for the biofilm growth.

Cyclic voltammetry (CV)

The quality of the tertiary bio-anode can be assessed
from CV curves recorded at day 10, when the current
was maximal. The scan rate of 10 mV/s was conse-
quently low enough to represent the stationary char-
acteristics of the electrode. The voltammograms
recorded in the absence of substrate confirmed that
the current was due to acetate oxidation. The voltam-
mograms (Fig. 8) of the sterile electrodes show a
hysteresis of the electrodes before use, due to gener-
ation of capacitive currents. As a consequence of the
increase of the interface capacitance with time, the

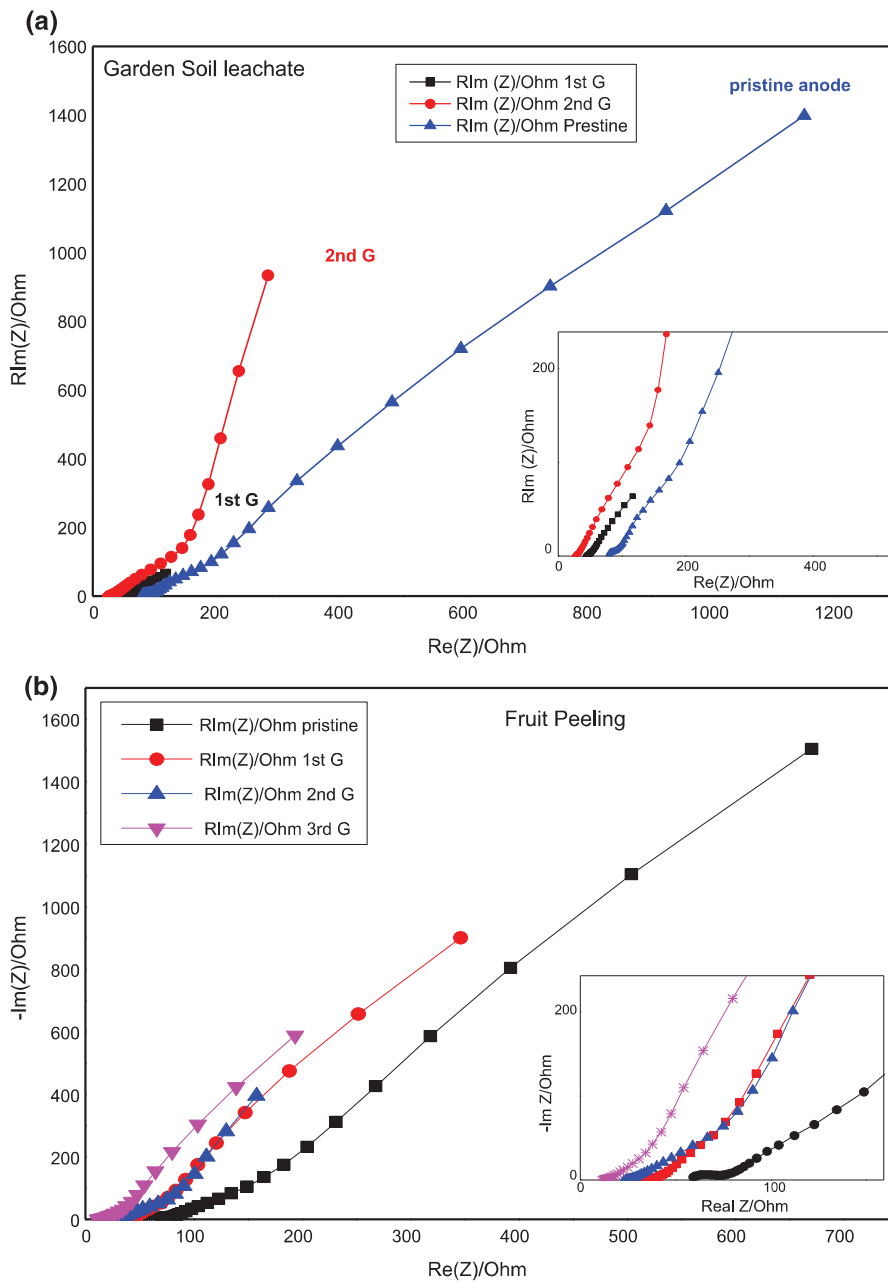


Fig. 7 **a** Impedance Nyquist diagram of different stages of bioanodes: pristine, 1st G and 2nd G of biofilm: GS. **b** Nyquist diagrams of bio-anodes inoculated with fruit peeling biofilms of:

Pristine/sterile leachate (black circle); 1st G (red circle); 2nd G and (blue inverted triangle); 3rd G (asterisk)

431 electron transfer also increases, as indicated by the
 432 voltammograms of the electrodes of 1st and 2nd Gs.
 433 These observations are in accordance with the voltam-
 434 mograms which give clearly the redox compounds

contained in the biofilms that can be addressed by the
 electrode (Fricke et al. 2008; Harnisch and Freguia
 2012).

435
 436
 437

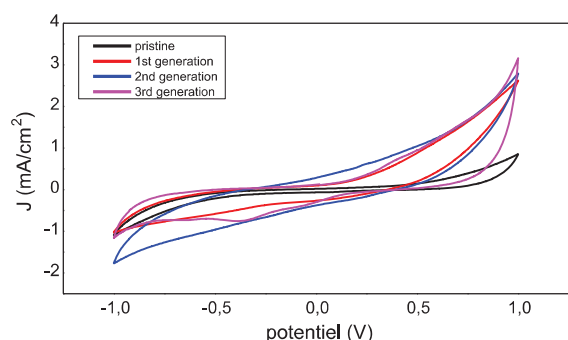


Fig. 8 Voltamograms of bio-anodes inoculated with FP biofilms of: Pristine/sterile leachate (black line); 1st G (red line); 2nd G (blue line); 3rd G (pink line)

438 Chemical oxygen demand (COD)

439 COD was determined for assessing the degradation of
 440 organic matter by MFC. In effect, its value for FP
 441 leachate before the treatment was about 466 mg L⁻¹.
 442 After 10 days, it decreased down to 147, 280 and
 443 345 mg L⁻¹ for 1st, 2nd and 3rd G FP, respectively.
 444 The corresponding COD abatements were, therefore
 445 tabulated by using (Eq. 1). The values are summarized
 446 in Table 2. As it is illustrated, the COD abatement was
 447 thus in favour to 1st FP-MFC, while the energy
 448 production was better with 2nd and 3rd Gs (i.e. after
 449 transplanting). The organic matter degradation was
 450 higher with scratched biofilm from the 1st G because
 451 the initial leachate contained not only the direct
 452 contact electrode biofilm but also planktonic microor-
 453 ganisms that helped in the COD abatement. In
 454 agreement with the results obtained recently using
 455 the MFC for the treatment of vinasse where the
 456 inoculum concentration promoted a different variation
 457 in relation to the measures of COD and power density
 458 (Ottoni et al. 2019).

$$\text{COD abatement (\%)} = 100 \times (C_i - C_f^G) / C_i \quad (1)$$

460 where C_i and C_f^G are the initial and final COD
 461 respectively.

Table 2 Values of COD abatement of FP-MFC for the three generations

| Generation | 1st G | 2nd G | 3rd G |
|-------------------|-------|-------|-------|
| COD abatement (%) | 68.45 | 39.91 | 25.96 |

Polarization and power characteristics of MFC

462
 463 The characteristic curves of polarization and power of
 464 the MFC were used to evaluate the electrical perform-
 465 ance of the cell under load. The polarization curve
 466 was obtained using different values of the resistance
 467 ranging between 10 Ω and 10 MΩ. As shown in Fig. 9,
 468 the polarization curve i.e. voltage versus current
 469 density presents three distinct regions. The first region
 470 represents the activation over voltage that results from
 471 the energy loss during the initiation of the Ox/Red
 472 reactions and electron transfer between the bacterial cell
 473 and the anodic surface. In the beginning, the MFC
 474 creates a short-circuit current density at the highest
 475 voltage. The second region shows an ohmic linear
 476 drop caused by the electrolyte. The third region
 477 displays a second over voltage that yields the maxi-
 478 mum open-circuit current density due to the loss of
 479 concentration occurring during the diffusion phe-
 480 nomenon. On the other hand, the power curve i.e.
 481 power density versus current density provides the
 482 maximum energy that can be delivered by the MFC.
 483 The power density is obtained as the product of output
 484 voltage and current density. The power density versus
 485 current density provides a curve having a first ohmic
 486 linear part, which increases by reaching the maximum
 487 power point. It then falls as the current density
 488 increases. As investigated in previous work, the power
 489 density of another MFC increased in the same manner
 490 with increasing values of current density, and reached
 491 optimal values upon the addition of substrate (Zer-
 492 rouki et al. 2018).

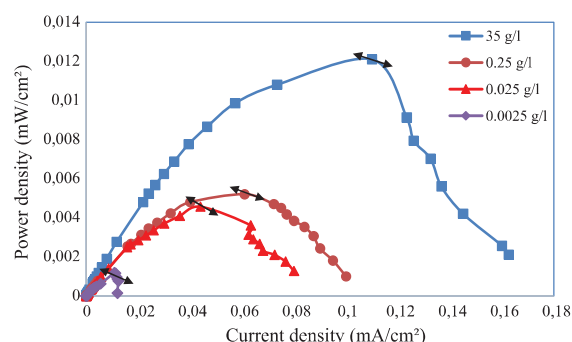


Fig. 9 Power density curves of MFCs using different concentrations of substrate (sodium acetate)

493 **Discussions**494 Comparison between three successive bio-film
495 generations

496 By using the scratched biofilm, it was possible to
497 reform an electro-active biofilm on a new electrode in
498 a sterilized medium. The comparison of the impe-
499 dance spectra and cyclic voltamograms of the sterile
500 electrode and the 2nd G biofilm electrode confirmed
501 the ability of the electroactive biofilm reformation on a
502 new support. Rivalland et al. (2015) reported that the
503 electrochemical monitoring of biofilm generations
504 collected from French Guiana mangrove sediments,
505 revealed the bacterial selection occurring at the anode
506 for three distinct generations. Indeed, the first biofilm
507 generation produced a stable current density reaching
508 about 18 A/m² while 2nd and 3rd Gs yielded current
509 densities of about 10 A/m², making in evidence that
510 the 1stG biofilm is more electroactive than the 2nd G
511 biofilm.

512 Besides, the importance of refreshing the medium
513 along with the addition of the fuel, was confirmed by
514 recorded higher voltage peaks. Ketep et al. (2014)
515 demonstrated that the bio-anodes formed upon the
516 addition of acetate, led to the highest current densities
517 (6 A/m²) but were then unable to oxidize the raw
518 effluent efficiently (0.5 A/m²). In contrast, the bio-
519 anodes formed without acetate addition, were fully
520 able to oxidize the organic matter contained in the
521 effluent, giving up to 4.5 A/m² in continuous mode.
522 Bacterial communities showed less bacterial diversity
523 for the acetate-fed bio-anodes compared to those
524 formed in raw effluents. By using the biofilm off-hook,
525 it was possible to reform an electro-active biofilm on a
526 new sterilized electrode in a sterilized medium.
527 Sedighi et al. (2018) investigated the relation between
528 the power generation of MFC and the COD removal in
529 optimised conditions. They concluded that optimising
530 both parameters simultaneously, made them compro-
531 mising and therefore reducing the MFC efficiency.

532 MFC-based bio-detector

533 MFC-based biosensors are considered to be the next
534 generation bio-sensing technology for environmental
535 monitoring (Sun et al. 2015), in particular the inclu-
536 sion of microbial activity, test of biochemical demand
537 and detection of toxicants (Yang et al. 2015).

538 Although small power output of MFC constraints its
539 application for directly operating electrical devices,
540 great progress has been achieved in its utilization as a
541 biosensor for monitoring of water quality and detect-
542 ing of air quality (Cui et al. 2019) as well as
543 determination of biodegradable organics (Lorant
544 et al. 2019). So, beyond the small energy production
545 harvested, our MFC was used also to develop a bio-
546 detector using a two-compartment cell. In the anode
547 compartment, the biocatalyst was renewed for each
548 sample analysis by substituting the old microbial
549 consortium with an equal amount of fresh one. The
550 sodium acetate substrate was utilized as a target for
551 detection. The biofilm was involved to degrade the
552 substrate by producing electrons to be used as source
553 of electric energy.

554 During the first week, the biofilm was cultured and
555 formed in the MFC inoculated with the initial
556 concentration of substrate 35 g/l. At the end of the
557 first experiment, the newly formed biofilm was well
558 recovered as needed on the same electrode. It was then
559 used to inoculate the new MFCs using disparate values
560 of substrate concentrations i.e. 0.0025, 0.025 and
561 0.25 g/l spanning more than fifteen thousands of order,
562 to ensure the low and high detection limits. These
563 limits were investigated by using values of maxima of
564 power density curves that highlight the performances
565 of the MFC.

566 As it is observed in Fig. 9, the peak of the
567 maximum power seems to be proportional to the
568 concentration of substrate consumed by the bacterial
569 consortium. Thus the MFC can play the role of
570 biosensor used as an organic matter detector. Besides,
571 in order to prove this detection, the variation of the
572 current density delivered by the MFC versus the fuel
573 concentration (sodium acetate) is plotted. Unfortu-
574 nately, it is shown to be not quite linear, because the
575 concentration range is too wide; values are of com-
576 pletely different orders of magnitude (35 g/l is 14 000
577 times higher than 0.0025 g/l). Hence, a logarithmic
578 scale plot yields a smooth straight which passes
579 approximately through all the data points. As shown in
580 Fig. 10, the straight line highlights the linearity of the
581 curve in logarithmic scale.

582 Furthermore, the MFC with replaceable consortium
583 could be used as a biosensor for on-line motoring of
584 organic matter as it has been previously highlighted by
585 Cui et al. (2019) and Sumaraj and Ghangrekar (2014).
586 As pointed out by Sun et al. (2019), more efforts are

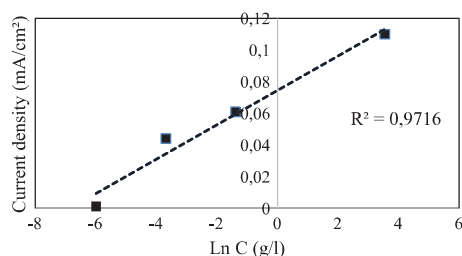


Fig. 10 Current density versus logarithm of concentration of substrate: a typical characteristic of biosensor

587 needed in the future to accelerate the response of the
588 biosensor. Following this recommendation, our MFC-
589 based detector may be accordingly successful for the
590 fulfilment of this requirement. This interesting biolog-
591 ical electric device has been tested using the micro-
592 organism from waste media, and used for detecting
593 organic matter detection, spanning the concentration
594 range 0.0025–35 g/l. It has, therefore, detected the
595 lowest concentration of substrate (i.e. 0.0025 g/l)
596 achieving the lowest current density 0.0011 mA/
597 cm². The higher the concentration, the more the
598 output current that is directly proportional to the
599 logarithm of the value of the input concentration (i.e.
600 0.11 mA/cm² at 35 g/l), hundred times greater. More-
601 over, according to Sun et al. (2019), the MFC-based
602 biosensor for selective monitoring of acetate during
603 anaerobic digestion, operated in a closed loop where
604 the increase in acetate concentration at the anode was a
605 function of the electric field generated by the MFC.
606 The resulted electric current obviously increased
607 linearly in the restricted concentration range of sodium
608 acetate, less than 20 mM (i.e. ≤ 1.65 g/l). However,
609 in our case, the current density was produced just by
610 injecting the substrate into the anode compartment. It
611 was really proportional to the logarithm of sodium
612 acetate concentration. As a consequence, the MFC
613 was able to detect wider concentration range of
614 sodium acetate (i.e. 0.0025–35 g/l). Our MFC could
615 therefore be used analogously in very wide concen-
616 tration range for detecting of organic matter, as well as
617 a radio frequency logarithmic detector power meter.

618 Conclusions

619 Taking our results into account, we can conclude that
620 the MFC technology is highly promising for the

621 treatment of wastewater and the production of low
622 bioenergy using two distinct inocula: Garden Soil and
623 Fruit Peeling. Furthermore, in the present investiga-
624 tion, we have demonstrated the possibility to improve
625 the energy production of a MFC by using different
626 biofilm generations. The scratching of the biofilm
627 from the electrode was achieved by ultrasound. Its re-
628 inoculation into a new leachate enhanced the energy
629 performance of the MFC using the 2ndG biofilm.
630 These results were confirmed by the impedance
631 spectra and the voltammograms. In addition, the
632 COD abatement was thus in favour to 1stG-MFC,
633 however, the energy production was better with 2nd &
634 3rd Gs, after biofilm transplantation. Besides, the
635 linearity of maximum current density versus concen-
636 tration of substrate on logarithmic scale makes in
637 evidence that the MFC could be used as a biosensor for
638 the detection of the waste organic matter. It can be
639 widely used in very wider concentration range detec-
640 tion for monitoring oxidation of matter, as it is the case
641 of logarithmic detector power meter for detecting
642 radio frequency signals.

Acknowledgements The authors are grateful to the financial
643 support from the cooperation Tassili scheme programme 14
644 MDU 912 in partnership between Algeria and France.
645

646 References

- Aiyer K, Vijayakumara BS (2019) Screening sediment samples
647 used as anolytes in microbial fuel cells for microbial
648 electron transfer activity using DREAM assay. *Biotechnol*
649 *Lett* 41(8–9):979–985. [https://doi.org/10.1007/s10529-](https://doi.org/10.1007/s10529-019-02704-3)
650 [019-02704-3](https://doi.org/10.1007/s10529-019-02704-3)
651
Akoğlu A (2020) The effect of some environmental conditions
652 on planktonic growth and biofilm formation by some lactic
653 acid bacteria isolated from a local cheese in Turkey.
654 *Biotechnol Lett* 42:481–492
655
Angelaalincy MJ, Navanietha Krishnaraj R, Shakambari G,
656 Ashokkumar B, Kathiresan S, Varalakshmi P (2018) Bio-
657 film engineering approaches for improving the perfor-
658 mance of microbial fuel cells and bioelectrochemical
659 systems. *Front Energy Res* 6:63
660
Cabezas A, Pommerenke B, Boon N, Friedrich MW (2015)
661 Geobacter, Anaeromyxobacter and Anaerolineae popula-
662 tions are enriched on anodes of root exudate-driven
663 microbial fuel cells in rice field soil. *Environ Microbiol*
664 *Rep* 7(3):489–497
665
Champavert J, Mardiana U, Innocent C (2017) Bio-catalytic
666 devices for energy production. *Curr Org Chem*
667 21(17):1702–1712. [https://doi.org/10.2174/](https://doi.org/10.2174/1385272821666170427155324)
668 [1385272821666170427155324](https://doi.org/10.2174/1385272821666170427155324)
669

- 670 Cheng S, Liu H, Logan BE (2006) Increased power generation
671 in a continuous flow MFC with advective flow through the
672 porous anode and reduced electrode spacing. *Environ Sci*
673 *Technol* 40(7):2426–2432
- 674 Cheng S, Kiely P, Logan BE (2011) Pre-acclimation of a
675 wastewater inoculum to cellulose in an aqueous-cathode
676 MEC improves power generation in air-cathode MFCs.
677 *Bioresour Technol* 102(1):367–371. <https://doi.org/10.1016/j.biortech.2010.05.083>
- 678 Cui Y, Lai B, Tang X (2019) Microbial fuel cell-based
679 biosensors. *Biosensors*. <https://doi.org/10.3390/bios9030092>
- 680 Doyle LE, Yung PY, Mitra SD, Wuertz S, Williams RBH, Lauro
681 FM, Marsili E (2017) Electrochemical and genomic analysis
682 of novel electroactive isolates obtained via potentiostatic
683 enrichment from tropical sediment. *J Power Sources*
684 356:539–548. <https://doi.org/10.1016/j.jpowsour.2017.03.147>
- 685 Fapetu S, Keshavarz T, Clements M, Kyazze G (2016) Contribution
686 of direct electron transfer mechanisms to overall electron
687 transfer in microbial fuel cells utilizing *Shewanella oneidensis*
688 cells as biocatalyst. *Biotechnol Lett* 38(9):1465–1473. <https://doi.org/10.1007/s10529-016-2128-x>
- 689 Fricke K, Harnisch F, Schröder U (2008) On the use of cyclic
690 voltammetry for the study of anodic electron transfer in
691 microbial fuel cells. *Energy Environ Sci* 1(1):144–147
- 692 Gorby YA, Yanina S, McLean JS, Rosso KM, Moyles D, Dohnalkova
693 A, Beveridge TJ, Chang IS, Kim BH, Kim KS, Culley DE, Reed SB,
694 Romine MF, Saffarini DA, Hill EA, Shi L, Elias DA, Kennedy DW,
695 Pinchuk G, Watanabe K, Ishii S, Logan B, Nealsen KH, Fredrickson
696 JK (2006) Electrically conductive bacterial nanowires produced
697 by *Shewanella oneidensis* strain MR-1 and other microorganisms.
698 *Proc Natl Acad Sci USA* 103(30):11358–11363
- 699 Harnisch F, Freguia S (2012) A basic tutorial on cyclic voltammetry
700 for the investigation of electroactive microbial biofilms. *Chemistry*
701 7(3):466–475
- 702 Huang L, Logan BE (2008) Electricity generation and treatment of
703 paper recycling wastewater using a microbial fuel cell. *Appl Microbiol
704 Biotechnol* 80(2):349–355. <https://doi.org/10.1007/s00253-008-1546-7>
- 705 Huang J, Wang Z, Zhu C, Ma J, Zhang X (2014) Wu Z (2014) Identification
706 of microbial communities in open and closed circuit bioelectrochemical
707 MBRs by high-throughput 454 pyrosequencing. *PLoS ONE* 9:e93842
- 708 Holmes DE, Nicoll JS, Bond DR, Lovley DR (2004) Potential role
709 of a novel psychrotolerant member of the family *Geobacteraceae*,
710 *Geopsychrobacter electrodiphilus* gen. nov., sp. nov. in electricity
711 production by a marine sediment fuel cell. *Appl Environ Microbiol*
712 70:6023–6030
- 713 Ketep SF, Bergel A, Bertrand M, Achouak W, Fourest E (2013) Lowering
714 the applied potential during successive scratching/re-inoculation
715 improves the performance of microbial anodes for microbial fuel
716 cells. *Bioresour Technol* 127:448–455. <https://doi.org/10.1016/j.biortech.2012.09.008>
- 717 Ketep SF, Bergel A, Bertrand M, Barakat M, Achouak W, Fourest E
718 (2014) Forming microbial anodes with acetate addition decreases
719 their capability to treat raw paper mill effluent. *Bioresour Technol*
720 164:285–291. <https://doi.org/10.1016/j.biortech.2014.04.088>
- 721 Kim JR, Jung SH, Regan JM, Logan BE (2007) Electricity generation
722 and microbial community analysis of alcohol powered microbial
723 fuel cells. *Biores Technol* 98(13):2568–2577
- 724 Kim M, Gutierrez-Cacciabue D, Schriever A, Rajal VB, Wuertz S
725 (2014) Evaluation of detachment methods for the enumeration of
726 *Bacteroides fragilis* in sediments via propidium monoazide
727 quantitative PCR, in comparison with *Enterococcus faecalis* and
728 *Escherichia coli*. *J Appl Microbiol* 117(5):1513–1522. <https://doi.org/10.1111/jam.12630>
- 729 Liu Y, Harnisch F, Fricke K, Sietmann R, Schröder U (2008) Improvement
730 of the anodic bioelectrocatalytic activity of mixed culture biofilms
731 by a simple consecutive electrochemical selection procedure. *Biosens
732 Bioelectron* 24(4):1006–1011. <https://doi.org/10.1016/j.bios.2008.08.001>
- 733 Lorant B, Gyalai-Korpos M, Goryanin I, Tardy GM (2019) Single
734 chamber air-cathode microbial fuel cells as biosensors for
735 determination of biodegradable organics. *Biotechnol Lett* 41(4–5):
736 555–563. <https://doi.org/10.1007/s10529-019-02668-4>
- 737 Manohar A, Manohar AK, Bretschger O, Nealsen KH, Mansfeld F
738 (2008) The use of electrochemical impedance spectroscopy (EIS)
739 in the evaluation of the electrochemical properties of a microbial
740 fuel cell. *Bioelectrochem* 72:149–154. <https://doi.org/10.1016/j.bioelechem.2008.01.004>
- 741 Mathuriya AS, Sharma VN (2009) Bioelectricity production from
742 paper industry waste using a microbial fuel cell by *Clostridium*
743 species. *J Biochem Technol* 1(2):49–52
- 744 Nam YS, Park TG (1999) Biodegradable polymeric microcellular
745 foams by modified thermally induced phase separation method.
746 *Biomaterials* 20:1783–1790
- 747 Ottoni CA, Simões MF, Santos JG, Peixoto L, Martins CR, Silva BP
748 et al (2019) Application of microbial fuel cell technology for
749 vinasse treatment and bioelectricity generation. *Biotech Lett*
750 41(1):107–114
- 751 Puig S, Serra M, Coma M, Balaguer MD, Colprim J (2011) Simultaneous
752 domestic wastewater treatment and renewable energy production
753 using microbial fuel cells (MFCs). *Water Sci Technol* 64(4):904–909
- 754 Rabaey K, Boon N, Siciliano SD, Verhaege M, Verstraete W (2004) Biofuel
755 cells select for microbial consortia that self-mediate electron
756 transfer. *Appl Environ Microbiol* 70(9):5373–5382
- 757 Rivalland C, Madhkour S, Salvin P, Robert F (2015) Electrochemical
758 and microbial monitoring of multi-generational electroactive
759 biofilms formed from mangrove sediment. *J Bioelectrochem*
760 106:125–132. <https://doi.org/10.1016/j.bioelechem.2015.05.011>
- 761 Santoro C, Arbizzani C, Erable B, Ieropoulos I (2017) Microbial
762 fuel cells: from fundamentals to applications: a review. *J Power
763 Sources* 356:225–244
- 764 Sedighi M, Aljlil SA, Alsubei MD, Ghasemi M, Mohammadi M (2018)
765 Performance optimisation of microbial fuel cell for wastewater
766 treatment and sustainable clean energy generation using response
767 surface methodology. *Alexandria Eng* 788

- 790 J 57(4):4243–4253. <https://doi.org/10.1016/j.aej.2018.02.012> 812
- 791 813
- 792 Sumaraj S, Ghangrekar MM (2014) Development of microbial 814
- 793 fuel cell as biosensor for detection of organic matter of 815
- 794 wastewater. *Recent Res Sci Technol* 6(1):162–166 816
- 795 Sun JZ, Kingori GP, Si RW, Zhai DD, Liao ZH, Sun DZ, Zheng 817
- 796 T, Yong YC (2015) Microbial fuel cell-based biosensors 818
- 797 for environmental monitoring: a review. *Water Sci Technol* 819
- 798 71:801–809. <https://doi.org/10.2166/wst.2015.035> 820
- 799 Sun H, Zhang Y, Wu S, Dong R, Angelidaki I (2019) Innovative 821
- 800 operation of microbial fuel cell-based biosensor for selec- 822
- 801 tive monitoring of acetate during anaerobic digestion. *Sci 823*
- 802 *Total Environ* 655:1439–1447. <https://doi.org/10.1016/j.scitotenv.2018.11.336> 824
- 803 825
- 804 Tingry S, Cretin M, Innocent C (2013) Les biopiles enzyma- 826
- 805 tiques pour produire de l'électricité. *l'actualité chimique* 827
- 806 373:18–25 828
- 807 Yahiaoui C, Kameche M, Innocent C, Khenifi A (2020) Con- 829
- 808 ception of yeast microbial desalination cell: applications to 812
- 809 dye wastewater treatment and lead removal. *Chem Eng 813*
- 810 *Commun.* <https://doi.org/10.1080/00986445.2020.1721479> 814
- 811 815
- Yang H, Zhou M, Liu M, Yang W, Gu T (2015) Microbial fuel 816
- cells for biosensor applications. *Biotechnol Lett* 817
- 37(12):2357–2364. <https://doi.org/10.1007/s10529-015-1926-7> 818
- Yates MD, Ma L, Sack J, Golden JP, Strycharz-Glaven SM, 819
- Yates SR, Tender LM (2017) Microbial electrochemical 820
- energy storage and recovery in a combined electrotrophic 821
- and electrogenic biofilm. *Environ Sci Technol Lett* 822
- 4(9):374–379. <https://doi.org/10.1021/acs.estlett.7b00335> 823
- Zhao C, Wu J, Ding Y, Wang VB, Zhang Y, Kjelleberg S, Loo 824
- JSC, Cao B, Zhang Q (2015) Hybrid conducting biofilm 825
- with built-in bacteria for high-performance microbial fuel 826
- cells. *Chemelectrochem* 2(2015):654–658 827
- Zerrouki A, Kameche M, Kebaili H, Boukoussa IS, Flitti MA, 828
- Ilikti H, Innocent C (2018) An investigation on polymer ion 829
- exchange membranes used as separators in low-energy 812
- microbial fuel cells. *Polym Bull* 75(11):4947–4965. <https://doi.org/10.1007/s00289-018-2305-2> 813

Publisher's Note Springer Nature remains neutral with regard to jurisdictional claims in published maps and institutional affiliations.